

Discovery of a Compact X-ray Source in the LMC Supernova Remnant N23 with *Chandra*

Asami Hayato^{1,2}, Aya Bamba², Toru Tamagawa^{2,1}, and Kiyoshi Kawabata¹

ABSTRACT

An X-ray compact source was discovered with *Chandra* in a supernova remnant (SNR) N23, located in the Large Magellanic Cloud. The compact source (CXOU J050552.3–680141) is seen in only the hard band (> 2 keV) image of N23, while the soft band image (< 2 keV) shows diffuse emission of the SNR, with an extent of $\sim 60'' \times 80''$. The compact source is located at almost the center of N23, and there is no identifiable object for the source from previous observations at any other wavelength. The source spectrum is best explained by a power-law model with a photon index of $\Gamma = 2.2^{+0.5}_{-0.3}$ and an absorption-corrected luminosity of $L_x = 1.0 \times 10^{34}$ ergs s⁻¹ in the 0.5–10 keV band for a distance of 50 kpc. Neither pulsation nor time variability of the source was detected with this observation with a time resolution of 3.2 sec. These results correspond with those of Hughes et al. (2006), who carried out analysis independently around the same time as our work.

Based on information from the best-fit power-law model, we suggest that the source emission is most likely from a rotation-powered pulsar and/or a pulsar wind nebula. It is generally inferred that the progenitor of N23 is a core-collapsed massive star.

Subject headings: ISM: supernova remnants — X-rays: individual (N23, CXOU J050552.3–680141)

1. Introduction

The Large Magellanic Cloud (LMC) quite well meet the requirements of a systematic study of supernova remnants (SNRs), in view of the facts concerning the known distance

¹Department of Physics, Faculty of Science, Tokyo University of Science, 1-3, Kagurazaka, Shinjyuku-ku, Tokyo 162-8601, Japan; hayato@crab.riken.jp

²RIKEN (Institute of Physical and Chemical Research), 2-1, Hirosawa, Wako, Saitama, 351-0198, Japan

(50 kpc; Feast 1999) and the small absorption because it is the nearest face-on galaxy to us. Over 30 SNRs have been discovered in the LMC so far, and categorized (Williams et al. 1999; Hughes et al. 1998). Besides, due to the limited spatial resolution of previous observations, it is reported that only six of pulsar/SNR associations in the LMC, PSR B0540–69 in N158A (Gotthelf & Wang 2000), PSR J0537–6910 in N157B (Marshall et al. 1998), a pulsar in N206 (Klinger et al. 2002), SGR 0526–66 in N49 (Kulkarni et al. 2003; Rothschild et al. 1994), XMMU J053559.3–673509 in DEM L241 (Bamba et al. 2006), and a pulsar wind nebula (PWN) in SNR B0453–68.5 (Gaensler et al. 2003a). A PWN is a synchrotron emission from high pressure plasma swept by the pulsar’s relativistic wind. Even though all of PWNe are powered by a pulsar, there is a case of a PWN without detection of a pulsar (Gaensler et al. 2003a). The pulsar/SNR or PWN/SNR associations provide meaningful information, such as the age of the systems, and the type of remnants.

The SNR N23 (0506–68.0) is one of the SNRs in the LMC that Milne et al. (1980) identified as an SNR with radio observations at 5 and 14.7 GHz for the first time. It is classified by its morphology as being a middle-aged (~ 3000 year) and an irregular-shaped SNR in Hughes et al. (1998). SNR N23 has not been well studied, so there is still no absolute solution for its explosion type (a core-collapse or a Ia). Cohen et al. (1988) insisted the possibility that N23 is a remnant from a massive star SN, since a CO cloud with high-density OB stars was observed within ~ 30 pc of N23. On the other hand, Banas et al. (1997) suggested that the remnant does not have any association with others according to their own observations with better spatial resolutions than that of the Cohen survey.

We present the results of an X-ray observation of N23 with *Chandra* in this paper. The observation details are summarized in §2, and the analysis results in §3. Using those results, we discuss the source discovered at the center of the remnant in §4, and §5 is a summary of this paper. Hughes et al. (2006) reported the same results based on their independent analysis.

2. Observation Details

An observation of SNR N23 was performed with the *Chandra* (Weisskopf et al. 2002) ACIS-S detector (Garmire et al. 2000) on December 29, 2002 (observation ID = 2762). The operation was in a timed exposure very faint mode, and it provided a time resolution of 3.24 sec. Data reduction was done using *Chandra* Interactive Analysis of Observation (CIAO) version 3.1 and CALDB version 2.28. From the Level 1 processed events that *Chandra* X-Ray Center gives, *Advanced Satellite for Cosmology and Astrophysics* (ASCA) grades of 0, 2, 3, 4, and 6 were selected. After that, the data was filtered for good time intervals and,

consequently, the total usable exposure time was 37 ksec.

3. Results

3.1. Image Analysis

Figure 1 shows ACIS X-ray images in the (a) 0.5–2.0 keV and (b) 2.0–8.0 keV bands. It demonstrates that the diffuse emission extend $\sim 60'' \times 80''$ (15 pc \times 19 pc for a distance of 50 kpc) in the soft X-ray band. The eastern part of the SNR is quite bright, whereas the northern and western parts are not. The lack of uniformity of the morphology might be due to a molecular cloud sitting southeast of N23 (Banas et al. 1997; Mathewson et al. 1985).

In the hard X-ray image, a compact source (CXOU J050552.3–680141) is found in the SNR, although diffuse emission is not. It was detected by the `wavdetect` command in CIAO with a significance of 11σ in the 2.0–8.0 keV band. The contour of 3σ detection has an elliptical shape ($1''.5 \times 1''.3$), and is slightly larger than the point spread function size at the source position of ACIS; however, it cannot be concluded that the source significantly extends, since there are non-uniform and complicated diffuse emissions over the source. Its location was identified as R.A. = $05^{\text{h}}05^{\text{m}}52^{\text{s}}.3$, decl. = $-68^{\circ}01'41''.2$ (J2000) with an uncertainty of less than a pixel size (0.5 arcsec). No counterpart object in this position has been found with the SIMBAD data base; in addition, there is no report about the compact source in either optical (Mathewson et al. 1985) or radio (Dickel & Milne 1998; Banas et al. 1997) band observations. An optical and a radio limits are magnitude > 17 and $< \sim 2\text{mJy}$ respectively (Hughes et al. 2006; Dickel & Milne 1998). We concentrate our discussion on this compact object in this paper, and call it “Source” hereinafter.

3.2. Spectral Analysis

We obtained the spectrum of Source with photons in the elliptical region at Source, described in §3.1 (Figure 1 (a)). There were 285 and 37 events in the region in the 0.5–2.0 keV and 2.0–8.0 keV bands, respectively, and the corresponding count rates were 4.4 and $0.57 \text{ counts sec}^{-1} \text{ arcmin}^{-2}$ with an exposure time of 37 ksec.

Because the background of Source surely consists of the thermal emission of SNR itself, we tested three backgrounds: the first was a circle that included the whole SNR (Bgd 1), the second was a circle from an extraneous region (Bgd 2), and the third was a circle that had almost the same surface brightness as the surrounding region of Source (Bgd 3), as shown

in Figure 1 (a).

We fitted three spectra with an absorbed power-law function, blackbody model, and plasma (Mekal) model (Mewe et al. 1985, 1986; Kaastra 1992; Liedahl et al. 1995), assuming that photons are absorbed in Galaxy ($N_{\text{H}}^{\text{gal}}$) and the LMC ($N_{\text{H}}^{\text{LMC}}$). The calculation of absorption columns was done using cross sections obtained by Morrison & McCammon (1983) for $N_{\text{H}}^{\text{gal}}$ and Balucinska-Church & McCammon (1992) for $N_{\text{H}}^{\text{LMC}}$, under the assumption that the abundances are 1 solar for $N_{\text{H}}^{\text{gal}}$ (Anders & Grevesse 1989) and 0.3 solar for $N_{\text{H}}^{\text{LMC}}$ (Russell & Dopita 1992; Hughes et al. 1998). We froze $N_{\text{H}}^{\text{gal}}$ to $5.6 \times 10^{20} \text{cm}^{-2}$ (Dickey & Lockman 1990), while we left $N_{\text{H}}^{\text{LMC}}$ a free parameter. Table 1 gives the results of the fittings. Even though we tested three models with three different background regions, it did not matter for the results of the absorption-corrected flux, $\sim 10^{-14} \text{ergs cm}^{-2} \text{s}^{-1}$. However, only the power-law fitting of the spectrum with the Bgd 1 gave an acceptable reduced χ^2 . Figure 2 represents the best-fit power-law model and data with Bgd 1.

3.3. Timing Analysis

Coherent pulsations of Source were searched. Selected photons are from the region of Source (see §3.2) and in the 2.0–8.0 keV band. The arrival times of photons were corrected with the `axbary` command in CIAO. Figure 3 gives a power-density spectrum of Source made based on a fast Fourier transform (FFT) algorithm. Even the highest peak does not protrude significantly from the white noise; thus, we consider that no significant pulsation was detected. Note that the time resolution of ACIS is only 3.24 sec in this observation.

We also searched for the time variability of Source. We made a light curve of the entire observation time, as demonstrated in Figure 4. A statistical analysis with the Kolmogorov-Smirnov test shows 53% for the probability of its constancy. As a result, we have concluded that Source has no significant time variability.

4. Discussion

Although a physical association between Source and the SNR N23 is strongly supported by the fact that the Source location is almost at the center of the SNR, our fitting results of the $N_{\text{H}}^{\text{LMC}}$ do not determine whether Source is in LMC or not due to the error. We thus verified the case that Source is (1) an object in Galaxy, (2) the object in LMC is unrelated with SNR, (3) a background active galactic nucleus (AGN), (4) the stellar remnant of N23.

4.1. If Source is in Galaxy

If Source is in Galaxy, possible candidates are an active RS CVn binary ($L_x=29-32$), a Cataclysmic Variables (CV; $L_x=30-33$), a Young Stellar Object (YSO; $L_x=29-31$), or a Low Mass X-ray Binary (LMXB; $L_x =30-39$), because their luminosities are consistent with the Source luminosity, assuming that Source is in Galaxy.

Since plasma models with any of three backgrounds did not provide an acceptable reduced χ^2 , we concluded that Source is unlikely to be a RS CVn, a CV, or a YSO, which are well explained by plasma models. The emission from a LMXB can explained by a power-law model, but the photon index is typically 1–2 (Muno et al. 2003), which is harder than the best-fit power-law model of Source.

As a result, we can say that Source would not be a considerable object in the case that Source is in Galaxy.

4.2. Source possibility of being a HMXB in the LMC

If Source is in the LMC and unrelated with the SNR, it could be a HMXB. The luminosity of HMXB ($\log L_x = 33-38$; Muno et al. 2003) corresponds to the luminosity of Source, if Source is in the LMC. The observed spectrum of a HMXB is explained with a photon index of 0.5–2.5 (Muno et al. 2003), which is also the same as the best-fit power-law of Source. However, the HMXB should be observed with the companion star in the optical band, and the expected optical limit of the companion star in the LMC is magnitude 16. The work by Hughes et al. (2006) using the data of the MACHO Project indicates that the optical limit in the Source region is > 17 . We can thus reject the possibility of being a HMXB in LMC.

4.3. Source possibility of being an AGN

The spectrum of an AGN has a photon index of $\sim 1-3$ (Beckmann et al. 2006), and the photon index of Source is in between. We calculated the expected number of AGNs in the back of N23 using a $\log N-\log S$ function measured by the *ROSAT* deep survey in the Lockman Hole (Hasinger et al. 1998). As a result, 24 AGNs, the flux of which is equal or higher than Source, are spread per square degree in the sky. Then, because the possibility of the AGN coincidence in the SNR region (elliptical; $\sim 60'' \times 80''$) is only 0.8%, we can hardly find an AGN in the back of N23.

4.4. Source as a stellar remnant of SNR N23

It is highly possible that Source associates with the SNR due to its location. The existence of an associating stellar remnant suggests that N23 is outcome of gravitational core-collapse of a massive star.

The possible candidates for Source as a stellar remnant of N23 would be a neutron star, a compact central object (CCO), an isolated pulsar, or a PWN.

The emission by a neutron star can be explained by a blackbody model with $kT = 0.15\text{--}0.25$ keV (Page and Sarmiento 1996; Page 1998), but the blackbody model was not able to represent the Source radiation with any backgrounds. Thus, Source is hardly said to be a usual neutron star.

CCOs have recently been discovered in several SNRs, like the central source in Cassiopeia A (Chakrabaty et al. 2001) or in Puppis A (Zavlin et al. 1999). CCOs' spectra can be fitted with either a blackbody or a power-law model, but the blackbody temperatures of CCOs are excessively high ($kT = \sim 0.3\text{--}0.6$ keV; Chakrabarty et al. 2001, Kaspi & Roberts 2004) to consider that they are the usual neutron stars; also, the photon indices of power-law fitting is too soft ($\Gamma = \sim 2.6\text{--}4.1$; Kaspi & Roberts 2004) to be pulsars. The luminosity of CCOs is $\log L_x = 31\text{--}35$ ergs s⁻¹, as shown by the triangle symbols in Figure 5. Even though the Source luminosity is consistent with those of CCOs, Source could not be acceptably fitted with a blackbody model, and the photon index of a power-law model is harder than the typical photon index of CCOs. Thus, we consider that Source in N23 seems not to be a CCO.

A pulsar typically has the power-law spectrum with a photon index of $\Gamma = \sim 0.6\text{--}1.9$ (Gotthelf & Wang 2000), which is harder than the best-fit photon index of Source. Meanwhile, for a PWN, we would observe a softer photon index, generically, $\Gamma = \sim 1.1\text{--}2.3$ (Cheng et al. 2004). The luminosity of the PWN is $\log L_x = 29\text{--}37$, which is brighter than that of only the pulsar (Cheng et al. 2004). This is indicated in Figure 5 by circle symbols. Due to the spectrum agreement, Source likely included the emission from a PWN. In this case, Source would be a rotation-powered pulsar plus a PWN, or a PWN powered by an unseen pulsar. For any conclusion, the pulsation searches with the better time resolution are required.

There is no counterpart of Source in the ATCA radio observation (1380, 2387, 4790, and 8640 MHz (Dickel & Milne 1998)), and the flux limit was estimated as ~ 2 mJy in any of four frequencies. Source is quite similar to the radio-quiet PWN around PSR B1509–58, which flux in the X-ray band is factor of 2 larger than Source and the radio flux limit is ~ 1.3 mJy (Gaensler et al. 2002, 1999). Therefore, the radio limit is consistent with our conclusion

that Source is a radio-quiet PWN.

5. Summary

A detailed analysis of the compact source at the center of SNR N23 in the LMC with *Chandra* has been presented. N23 has $\sim 60'' \times 80''$ diffuse emission in the < 2 keV band, and an almost point-like compact source in the > 2 keV band. This source (CXOU J050552.3–680141) has no counterpart at any other wavelength. The spectrum of the source can be fitted to a power-law function with $\Gamma = 2.2^{+0.5}_{-0.3}$, and a luminosity of 1.0×10^{34} ergs s^{-1} in the 0.5–10 keV band for a distance of 50 kpc. Neither significant pulsation nor time variability was detected with the time resolution of 3.2 sec observation. The results of the fittings indicate that the source might well be a rotation-powered pulsar and/or a pulsar wind nebula (PWN) associating with the SNR. It implies that the progenitor of the remnant is likely to be a massive star.

We gratefully acknowledge the *Chandra* team for making available its public data used herein. We thank R. Yamazaki, K. Mori, T. Mihara, M. Nakajima, N. Isobe and K. Makishima for their fruitful discussions. This research made use of the SIMBAD data base, obtained by CDS, Strasbourg, France. This work is supported in part by the Grant-in-Aid for Young Scientists (B) of the Ministry of Education, Culture, Sports, Science and Technology (No.17740183).

REFERENCES

- Anders, E., & Grevesse, N., *Geochimia et Cosmochimica Acta*, 53, 197
- Balucinska-Church, M., & McCammon, D. 1992, *ApJ*, 400, 699
- Bamba, A., Ueno, M., Nakajima, H., Mori, K., & Koyama, K. 2006, *A&A*, 450, 585
- Banas, K. R., Hughes, J. P., Bronfman, L., & Nyman, L. 1997, *ApJ*, 480, 607
- Beckmann, V., Gehrels, N., & Shrader, C. R. 2006, *ApJ*, 638, 642
- Caraveo, P. A., Bignami, G. F., DeLuca, A., Mereghetti, S., Pellizzoni, A., Mignani, R., Tur, A., & Becker, W. 2003, *Science*, 301, 1345
- Chakrabarty, D., Pivovarov, M. J., Hernquist, L. E., Heyl, J. S., & Narayan, R. 2001, *ApJ*, 548, 800

- Cheng, K. S., Taam, R. E., & Wang, W. 2004, *ApJ*, 617, 480
- Cohen, R. S., Dame, T. M., Montani, J., Rubio, M., & Thaddeus, P. 1988, *ApJ*, 331, L95
- Dickel, J. R., & Milne, D. K. 1998, *ApJ*, 115, 1057
- Dickey, J. M., & Lockman, F. J. 1990, *ARA&A*, 28, 215
- Finley, J. P., Srinivasan, R., Saito, Y., Hirayama, M., Kamae, T., & Yoshida, K. 1998, *ApJ*, 493, 884
- Frail, D. A. & Scharringhausen, B. R. 1997, *ApJ*, 480, 364
- Gaensler, B. M., Arons, J., Kaspi, V. M., Pivovarov, M. J., Kawai, N., & Tamura, K. 2002, *ApJ*, 569, 878
- Gaensler, B. M., Brazier, K. T. S., Manchester, R. N., Johnston, S., & Green, A. J. 1999, *MNRAS*, 305, 724
- Gaensler, B. M., Hendrick, S. P., Reynolds, S. P., & Borkowski, K. J. 2003a, *ApJ*, 594, L111
- Gaensler, B. M., Schulz, N. S., Kaspi, V. M., Baganoff, W. E. 2003b, *ApJ*, 588, 411
- Gaensler, B. M., Stappers, B. W., Frail, D. A., Moffett, D. A., Johnston, S., & Chatterjee, S. 2000, *MNRAS*, 318, 58
- Gaensler, B. M., Swaluw, E. V. D., Camilo, F., Kaspi, V. M., Baganoff, F. K., Yusef-Zadeh, F., & Manchester, R. N. 2004, *ApJ*, 616, 383
- Garmire, G., Feigelson, E. D., Broos, P., Hillenbrand, L. A., Pravdo, S. H., Townsley, L., & Tsuboi, Y. 2000, *AJ*, 120, 1426
- Gotthelf, E. V., & Kaspi, V. M. 1998, *ApJ*, 497, L29
- Gotthelf, E. V., Petre, R., & Vasisht, G. 1999, *ApJ*, 514, L107
- Gotthelf, E. V., & Vasisht, V. 1997, *ApJ*, 486, L133
- Gotthelf, E. V., & Wang, D. 2000, *ApJ*, 532, L117
- Halpern, J. P., Camilo, F., Gotthelf, E. V., Helfand, D. J., Kramer, M., Lyne, A. G., Leighly, K. M., & Eracleous, M. 2001, *ApJ*, 552, L125
- Hasinger, G., Burg, R., Giacconi, R., Schmidt, M., Trümper, J., & Zamorani, G. 1998, *A&A*, 329, 482

- Hessels, J. W. T., Roberts, M. S. E., Ranson, S. M., Kaspi, V. M., Romani, R. W., Ng, C-Y, Freire, P. C. C., & Gaensler, B. M. 2004, *ApJ*, 612, 389
- Hughes, J. P., Hayashi, I., & Koyama, K. 1998, *ApJ*, 505, 732
- Hughes, J. P., Slane, P. O., Burrows, D. N., Garmire, G., Nousekm J. A., Olbert, C. M., & Keohane, J. W. 2001, *ApJ*, 559, L153
- Hughes, J. P., Rafelski, M., Warren, J. S., Rakowski, C., Slane, P., Burrows, D., & Nousek, J. 2006, *ApJ*, 645, L117
- Kaaret, P., Marshall, H. L., Alodcroft, T. L., Graessle, D. E., Karovska, M., Murray, S. S., Rots, A. H., Schulz, N. S., & Seward, F. D. 2001, *ApJ*, 546, 1159
- Kaastra, J. S., 1992, An X-ray Spectral Code for Optically Thin Plasmas (Internal SRON-Leiden Report, updated version 2.0)
- Kaspi, V. M., Gotthelf, E. V., Gaensler, B. M., & Lyutikov, M. 2001, *ApJ*, 562, L163
- Klinger, R. J., Dickel, J. R., & Fields, B. D. 2002, *ApJ*, 124, 2135
- Kulukarni, S. R., Kaplan, D. L., Marshall, H. L., Frail, D. A., Murakami, T., & Yonetoku, D. 2003, *ApJ*, 585, 948
- Lideahl, D. A., Osterheld, A. L., & Goldstein, W. M. 1995, *ApJ*, 438, 115
- Lu, F. J., Wang, Q. D., Aschenbach, B., Durouchoux, P., & Song, L. M. 2002, *ApJ*, 568, L49
- Milne, D. K., Caswell, L., & Haynes, R. F. 1980, *MNRAS*, 191, 469
- Mathewson, D. S., Ford, V. L., Tuohy, I. R., Mills, B. Y., Turtle, A. J., & Helfand, D. J. 1985, *ApJS*, 58, 197
- Marshall, F. E., Gotthelf, E. V., Zhang, W., Middleditch, J., & Wang, Q. D. 1998, *ApJ*, 499, L179
- Mereghetti, S., Bignami, G. F., & Caraveo, P. A. 1996, *ApJ*, 464, 842
- Mereghetti, S., Tiengo, A., & Israel, G. L. 2002, *ApJ*, 569, 275
- Mewe, R., Gronenschild, E. H. B. M., & van den Oord, G. H. J. 1985, *A&AS*, 62, 97
- Mewe, R., Lemen, J. R., & van den Oord, G. H. J. 1986, *A&AS*, 65, 511

- Morrison, D. S., & McCommon, D. 1983, *ApJ*, 270, 119
- Muno, M. P., Baganoff, F. K., Baytz, M. W., Brandt, W. N., Broos, P. S., Feigelson, E. D., Garmire, G. P., Morris, M. R., Ricker, G. R., & Townsley L. K. 2003, *ApJ*, 589, 225
- Murray, S. S., Slane, P. O., Seward, F. D., & Ransom, S. M. 2002, *ApJ*, 568, 226
- Page, D. 1998, in *The many Faces of Neutron Stars*, ed. R. Buccheri, J. van Paradijs, & M. A. Alpar (Dordrecht:Kluwer), 539
- Page, D., & Sarmiento, A. 1996, *ApJ*, 473, 1067
- Pavlov, G. G., Sanwal, D., Kiziltan, B., & Garmire, G. P. 2001, *ApJ*, 559, L131
- Petre, R., Becker, C. M., & Winkler, P. F. 1996, *ApJ*, 465, L43
- Petre, R., Kuntz, K. D., & Shelton, R. L. 2002, *ApJ*, 579, 404
- Roberts, M. S. E., Tam, C. R., Kaspi, V. M., & Lyutikov, M. 2003 *ApJ*, 588, 992
- Rothschild, R. E., Kulkarni, S. R., & Lingenfelter, R. E. 1994, *Nature*, 368, 432
- Russell, S. C., & Dopita, M. A. 1992, *ApJ*, 384, 508, *Nature*, 368, 432
- Safi-Harb, S., Ögelman, H., & Finley, J. P. 1995, *ApJ*, 439, 772
- Stappers, B.W., Gaensler, B. M., Kaspi, V. M., van der Klis, M., & Lewin, H. W. G. 2003, *Science*, 299, 1372
- Torii, K., Slane, P. O., Kinigasa, K., Hashimoto, K., & Tsunemi, H. 2000, *PASJ*, 52, 875
- Wang, Q. D., & Gotthelf E. V. 1998 *ApJ*, 494, 134
- Weisskopf, M. C., Brinkman, B., Canizares, C., Garmire, G., Murray, S., & Van Speybroeck, L. P. 2002, *PASP*, 114, 1
- Williams, R. M., Chu, Y. H., Dickel, J. R., Petre, R., Smith, R. C., & Tavaréz, M. 1999, *ApJS*, 123, 467
- Zavlin, V. E., Trümper, J., & Pavlov, G. G. 1999, *ApJ*, 525, 959

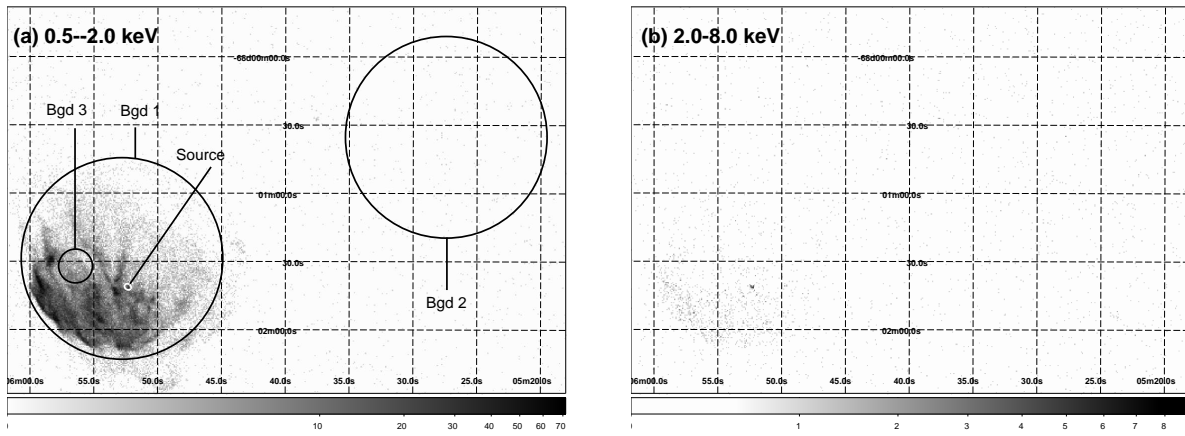


Fig. 1.— *Chandra* ACIS X-ray images of SNR N23 in the (a) 0.5–2.0 keV and (b) 2.0–8.0 keV bands in a logarithmic scale. The source and background regions are shown in the panel (a). The coordinates are in J2000.

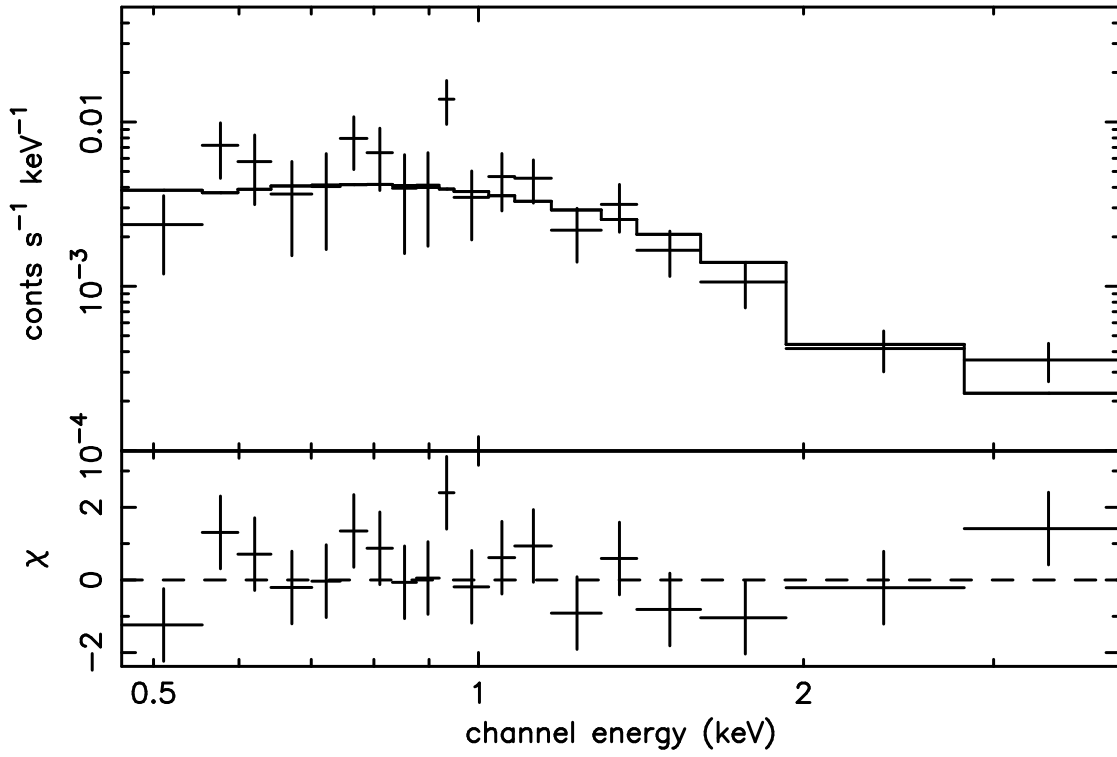


Fig. 2.— The background (Bgd 1) subtracted spectrum of the source (crosses) with the best fit model, the power-law function (solid line). Residuals are shown in the bottom panel.

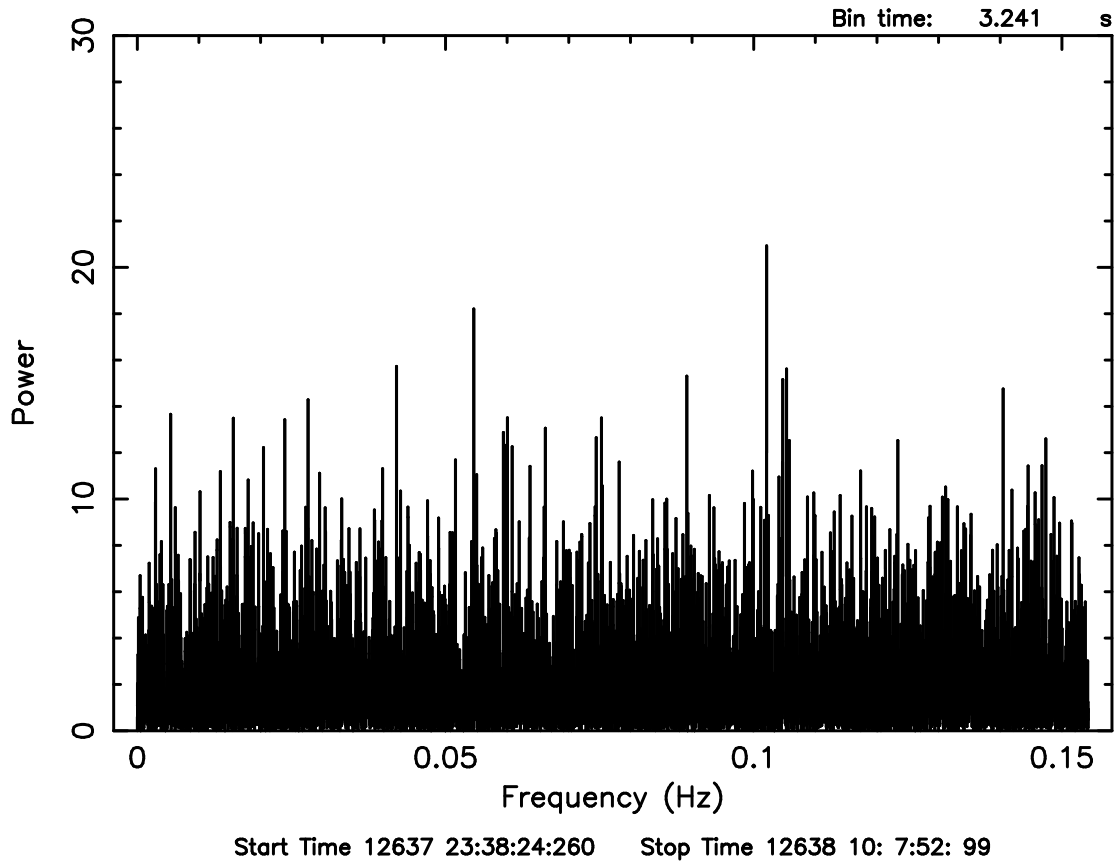


Fig. 3.— The power spectrum of Source in the 2.0–8.0 keV band.

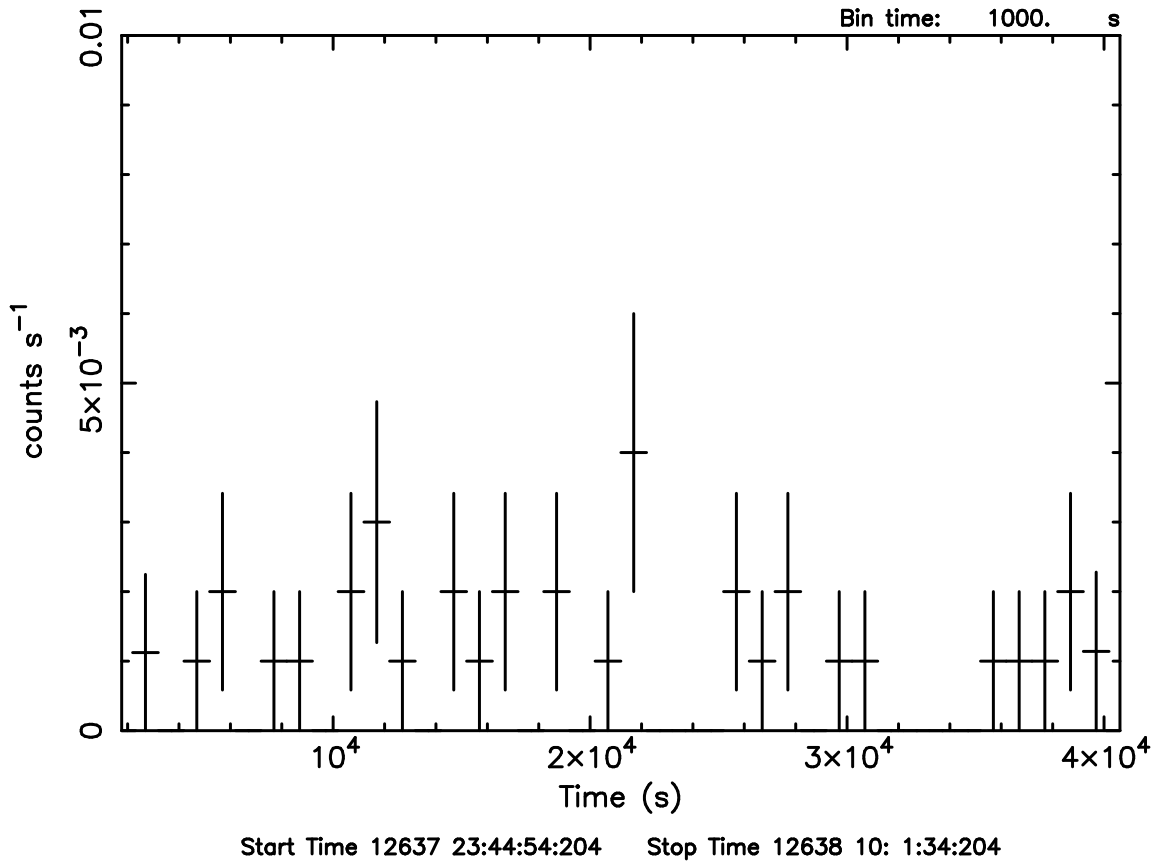


Fig. 4.— The X-ray light curve of Source in the 2.0–8.0 keV band, binned with 1000 s. The background is not subtracted.

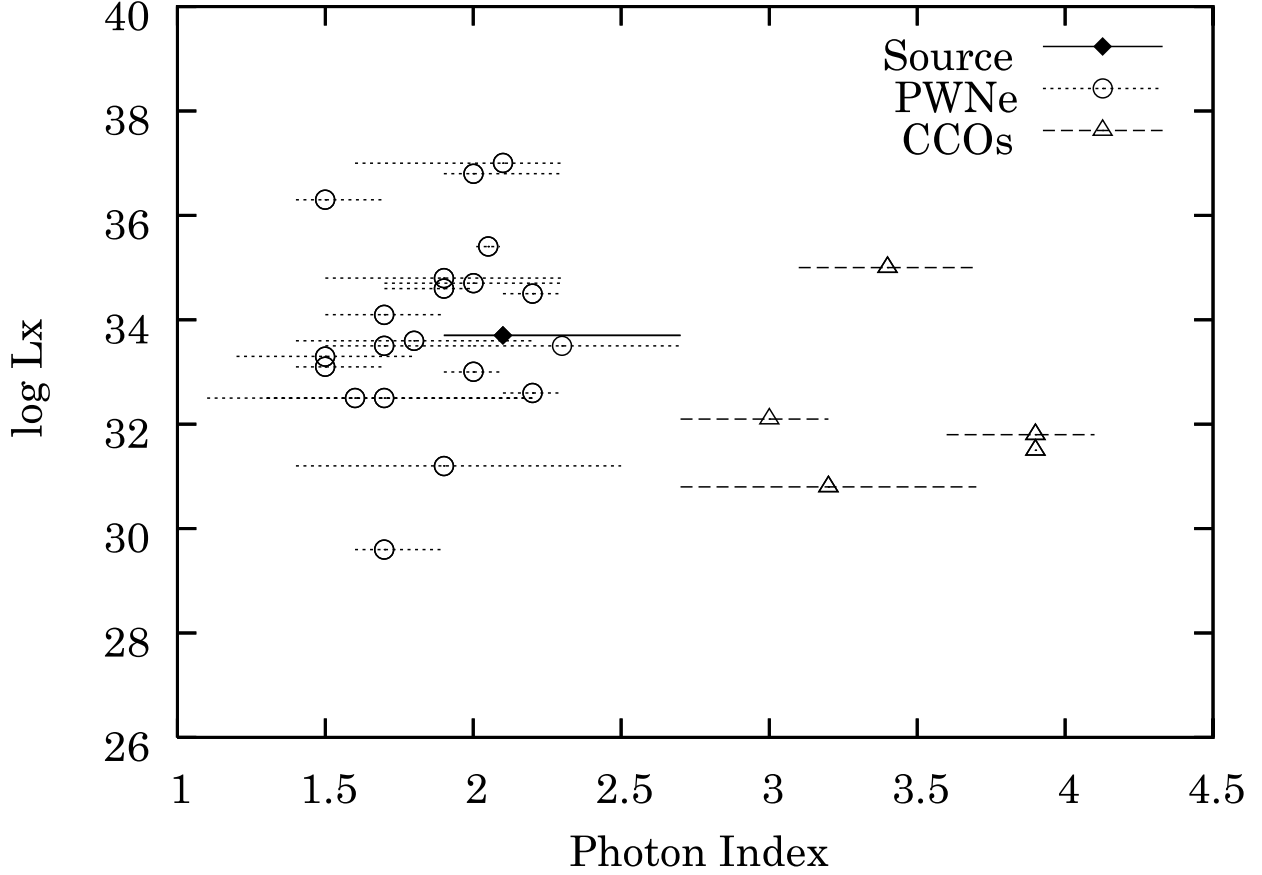


Fig. 5.— Relationships of photon indices and luminosities of Source (a solid line with a diamond), PWNe (dotted lines with circles), and CCOs (dashed lines with triangles). Referred PWNe are in SNR G18.0-0.7 (assumed distance $D = 4$ kpc; Gaensler et al. (2003b)), in N157B ($D = 50$ kpc; Marshall et al. (1998); Wang and Gotthelf (1998)), PSR B0540–69 ($D = 50$ kpc; Kaaret (2001)), in G11.2-0.3 ($D = 5.0$ kpc; Roberts et al. (2003)), Crab ($D = 2.0$ kpc; Petre et al. (2002)), Vela ($D = 0.3$ kpc; Pavlov et al. (2001)), Geminga ($D = 0.16$ kpc; Caraveo et al. (2003)), PSR J2229+6114 ($D = 3.0$ kpc; Halpern et al. (2001)), PSR 1105–6107 ($D = 7$ kpc; Gotthelf & Kaspi (1998)), PSR 1706–44 ($D = 2.5$ kpc; Finley et al. (1998)), PSR B1757–24 ($D = 5$ kpc; Kaspi et al. (2001)), in 3C58 ($D = 2.6$ kpc; Murray et al. (2002); Torii et al. (2000)), PSR B1957+20 ($D = 1.5$ kpc; Stappers et al. (2003)), PSR J2021+3651 ($D = 10$ kpc; Hessels et al. (2004)), PSR J1747–2958 ($D = 5$ kpc; Gaensler et al. (2004)), in SNR G292.0+1.8 ($D = 4.8$ kpc; Hughes et al. (2001)), in W44 ($D = 2.02$ kpc; Petre et al. (2002)), PSR J1930+1852 ($D = 5$ kpc; Lu et al. (2002)), PSR B0458–685 ($D = 50$ kpc; Gaensler et al. (2004)), and PSR B1509–58 ($D = 5.2$ kpc; Gaensler et al. (2002)). The PWNe list of Cheng et al. (2004) are used. CCOs are in Cas A ($D = 3.4$ kpc; Mereghetti et al. (2002)), in G226.2–1.2 ($D = 0.4$ kpc; Pavlov et al. (2001)), in G296.5+10.0 ($D = 1.5$ kpc; Mereghetti et al. (1996)), in RCW 103 ($D = 3.3$ kpc; Gotthelf et al. (1999)), and in Kes 73 ($D = 7.0$ kpc; Gottelf & Vasisht (1997)). Error bars indicate 90% confidence.

Table 1: Best-fit parameters for Source^a

Power-law ^b	Γ		$N_{\text{H}}^{\text{LMCc}}$ [10^{20}cm^{-2}]	Flux ^d [ergs $\text{cm}^{-2} \text{s}^{-1}$]	$\chi^2/\text{d.o.f.}$
with Bgd 1	2.2 (1.9–2.7)		<0.32	3.5×10^{-14}	18.4/16
with Bgd 2	3.7 (3.0–4.8)		0.4 (0.1–0.9)	7.0×10^{-14}	37.9/16
with Bgd 3	2.4 (1.9–2.7)		<39.2	3.7×10^{-14}	20.5/16
Blackbody ^b	kT [keV]		$N_{\text{H}}^{\text{LMCc}}$ [10^{20}cm^{-2}]	Flux ^d [ergs $\text{cm}^{-2} \text{s}^{-1}$]	$\chi^2/\text{d.o.f.}$
with Bgd 1	0.26 (0.22–0.32)		<0.2	2.0×10^{-14}	34.7/16
with Bgd 2	0.20 (0.18–0.22)		<0.2	3.3×10^{-14}	47.7/16
with Bgd 3	0.27 (0.24–0.29)		<0.4	2.0×10^{-14}	36.7/16
Plasma ^b	kT [keV]	Abundance	$N_{\text{H}}^{\text{LMCc}}$ [10^{20}cm^{-2}]	Flux ^d [ergs $\text{cm}^{-2} \text{s}^{-1}$]	$\chi^2/\text{d.o.f.}$
with Bgd 1	1.63 (1.11–4.84)	<1.0	<0.2	2.6×10^{-14}	22.2/15
with Bgd 2	0.65 (0.50–0.80)	<0.052	<5.2	3.6×10^{-14}	35.1/15
with Bgd 3	1.63 (0.83–2.60)	<0.3	<0.2	2.7×10^{-14}	24.2/15

^aValues in parentheses are 90% parameters confidence regions.

^bThe assumed $N_{\text{H}}^{\text{gal}}$ was $5.6 \times 10^{20} \text{cm}^{-2}$ (Dickey & Lockman 1990).

^cIn the 0.5–10 keV band. Corrected for absorption.

^d0.3 solar abundance are used.